Pure & Appl. Chem., Vol. 62, No. 5, pp. 877–887, 1990.
Printed in Great Britain.

Numerical simulation of flames: current status and future perspectives

Elaine S. Oran

Laboratory for Computational Physics and Fluid Dynamics
Naval Research Laboratory, Washington, DC, 20375

Abstract – The fundamental difficulties that arise in numerically modeling the behavior of flames are due both to the number and complexity of the contributing physical processes and the availability of accurate enough input data. Both of these issues must be addressed to obtain calculations accurate enough to give quantitatively correct predictions. This paper describes our current status of detailed time-dependent numerical models of laminar flames by describing some of the numerical algorithms representing the relevant physical processes and some of the types of systems that have been modeled. Examples are taken from simulations of premixed hydrogen-oxygen flames, ranging in complexity from one-dimensional laminar flames to two-dimensional unstable transitional flames. Future directions of the development and application of these models are discussed.

INTRODUCTION

A model of a flame requires combining representations of a number of physical and chemical processes. At the simplest level of flame modeling, accurate algorithms are required to represent convection, molecular diffusion, thermal conduction, and chemical reactions with subsequent heat release. Such a model, with appropriate terms to describe heat loss to the surroundings, might suffice to describe a near-stoichiometric laminar hydrogen-oxygen flame. In more complicated cases, algorithms for thermal diffusion, radiation transport, and multiphase flow processes must also be included. In some regimes of the flame, certain of these processes are not important and can therefore be ignored. However, sometimes the importance of a specific process is not understood *a priori* and it can be misleading to omit it in the calculation. In some cases, resolving one particular process can be a formidable task. Consider, for example, the futility of trying to resolve all of the time and space scales of a high-speed turbulent flow, or the cost of including all of the chemical reactions in a nonequilibrium hydrocarbon oxidation process.

The approach we have taken to simulating flames has been to use the best or most appropriate numerical algorithm we can find or invent to describe each type of physical process, and then to couple these by timestep-splitting techniques. This provides the flexibility of being able to change the level of accuracy or detail of a particular submodel. Thus the model for a low-gravity laminar flame can have the same general structure as that for a ramjet engine. However, the level of description of a key physical process might be different, or a representation of an additional process may be added to or removed from the model in an orderly way.

This paper first describes the current status of detailed numerical simulations of time-dependent gas-phase laminar and transitional flames. Selected algorithms are described briefly or referenced, and then selected examples of flame calculations are shown from simulations performed at the Naval Research Laboratory. These examples range in complexity from extremely detailed descriptions of laminar premixed flames to complex multidimensional flame structures in a ramjet engine. Future extensions of this work and new directions are described in terms of the quickly evolving computational technology that is becoming available. Much of the work described in this paper is described more fully and with a more complete set of reference in ref. 1.

GOVERNING EQUATIONS

The equations used to model neutral gas-phase reactive flows are the continuum time-dependent equations for conservation of mass density ρ, individual chemical species number densities, $\{n_i\}$, momentum density $\rho\mathbf{v}$, and total energy E,

$$\frac{\partial \rho}{\partial t} = -\nabla \cdot (\rho \mathbf{v}), \tag{1}$$

$$\frac{\partial n_i}{\partial t} = -\nabla \cdot (n_i \mathbf{v}) - \nabla \cdot (n_i \mathbf{v}_{di}) + Q_i - L_i n_i, \qquad i = 1, \ldots N_s, \tag{2}$$

$$\frac{\partial \rho \mathbf{v}}{\partial t} = -\nabla \cdot (\rho \mathbf{v}\mathbf{v}) - \nabla \cdot \mathbf{P} + \sum_i \rho_i \mathbf{a}_i, \tag{3}$$

and

$$\frac{\partial E}{\partial t} = -\nabla \cdot (E\mathbf{v}) - \nabla \cdot (\mathbf{v} \cdot \mathbf{P}) - \nabla \cdot (\mathbf{q}) + \mathbf{v} \cdot \sum_i m_i \mathbf{a}_i + \sum_i \mathbf{v}_{di} \cdot m_i \mathbf{a}_i \,. \tag{4}$$

The first term on the right hand side of each of these equations describes the convective fluid dynamics effects. The remaining terms contain the source, sink, coupling, external force, and diffusive transport terms that drive the fluid dynamics. Pressure is a tensor,

$$\mathbf{P} \equiv P(N,T)\mathbf{I} + \left(\frac{2}{3}\mu - \kappa\right)(\nabla \cdot \mathbf{v})\mathbf{I} - \mu[(\nabla \mathbf{v}) + (\nabla \mathbf{v})^T] \,, \tag{5}$$

where μ and κ are the shear and bulk viscosity coefficients and the superscript T means matrix transpose. The heat flux, $\mathbf{q}$, total number density, N, and internal energy density, ϵ, can be found from

$$\mathbf{q}(N,T) \equiv -\lambda_m \nabla T + \sum_i n_i h_i \mathbf{v}_{di} + P \sum_i K_i^T \mathbf{v}_{di} + \mathbf{q}_r, \tag{6}$$

$$N \equiv \sum_i n_i, \tag{7}$$

and

$$E \equiv \frac{1}{2}\rho \mathbf{v} \cdot \mathbf{v} + \rho\epsilon. \tag{8}$$

Here K_i^T is the thermal diffusion coefficient of species i, λ_m is the mixture thermal conductivity, $\mathbf{v}_{di}$ is the diffusion velocity for species i, $\mathbf{q}_r$ is the heat flux due to radiation, and h_i is the specific enthalpy. For the flames we are discussing, the external force is gravity, so that the accelerations are the same for the individual species present, $\mathbf{a}_i = \mathbf{g}$. In addition, we need equations of states which for a gas at normal temperature and pressures we usually take as

$$P = N k_B T = \rho R T \,, \tag{9}$$

$$h_i = h_{io} + \int_{T^\circ}^{T} c_{pi}\, dT \,, \tag{10}$$

Table 1. Terms in the Reactive Flow Equations

$\frac{\partial \rho}{\partial t} = \gamma\rho + S$	Local Processes: Source, Sink, Coupling, Chemical Reactions
$\frac{\partial \rho}{\partial t} = \nu \nabla^2 \rho$	Diffusive Processes: Molecular Diffusion, Thermal Conduction, Thermal Diffusion
$\frac{\partial \rho}{\partial t} = -\nabla \cdot (\rho \mathbf{v})$	Convective Processes: Advection, Compression, Rotation
$\frac{\partial^2 \rho}{\partial t^2} = c_w^2 \nabla^2 \rho$	Waves and Oscillations: Sound Waves, Gravity Waves, Oscillations

where h_{io} and c_{pi} are the heat of formation and specific heat of species i. Note that a great deal of information has been hidden in the chemical production terms and loss rates, $\{Q_i\}$ and $\{L_i\}$, which can be complicated functions of of temperature, pressure, and the other species densities.

The set of species diffusion velocities $\{\mathbf{v}_{di}\}$ are found by inverting the matrix equation

$$\mathbf{W}_i = \sum_k \frac{n_i n_k}{N^2 D_{ik}} (\mathbf{v}_{dk} - \mathbf{v}_{di}), \tag{11}$$

where the source terms $\{\mathbf{W}_i\}$ in Eq. (11) are defined as

$$\mathbf{W}_i \equiv \nabla\left(\frac{n_i}{N}\right) - \left(\frac{\rho_i}{\rho} - \frac{n_i}{N}\right)\frac{\nabla P}{P} - K_i^T \frac{\nabla T}{T} \,. \tag{12}$$

The diffusion velocities are subject to the constraint

$$\sum_i \rho_i \mathbf{v}_{di} = 0. \tag{13}$$

This is an extremely rich set of equations. Combined with appropriate initial and boundary conditions, these equations describe, for example, flames, detonations, or turbulence. There are basically four types of physical processes in this set of equations, and these are summarized in Table 1. The first two, chemical reactions and diffusive transport, originate in the atomic and molecular nature of matter. The third and fourth, convection and wavelike properties, are collective phenomena.

Chemical reactions (or chemical kinetics), represented by the production and loss terms, Q_i and $L_i n_i$ in Eq. (2), are an example of "local" phenomena which do not depend on spatial gradients. Other examples of local phenomena are phase changes, external source terms such as laser or spark heating, and sinks such as optically thin radiation loss. The macroscopic models of these processes used in the continuum equations arise from averages over microscopic effects. Diffusion (or diffusive transport), has the general form $\nabla \cdot Y$ where Y may be $n_i v_{di}$, $\mu \nabla v$, or q. The last two terms in Eq. (5) describe the diffusive effects of viscosity. The last terms in Eq. (6) describe the change in energy due to molecular diffusion, chemical reactions, and radiation transport. The third equation in Table 1 is a continuity equation describing convection. Convection effects are represented in the equations by fluxes of conserved quantities through volumes, e.g., $\nabla \cdot vX$ where X is ρ, n_i, E, ρv or P. Convection is a continuum concept, which assumes that quantities such as density, velocity, and energy are smoothly varying functions of position. The fluid variables are defined as averages over the actual particle distributions, so only a few degrees of freedom are necessary to describe the local state of the material. Wavelike and oscillatory behavior are described implicitly in the reactive flow equations by coupled continuity equations. The important point about wave motion is that energy can be carried throughout the system without convective fluid or particle motions. It is transferred from one element of the fluid to others by waves that can travel much faster than the fluid. The main type of waves considered are shock waves, which move as discontinuities through the system, and sound waves, in which there are alternating compressions and rarefactions in density and pressure of the fluid. Other types of waves included in these reactive flow equations are gravity waves and chemical reaction waves.

The complete set of reactive flow equations is so difficult to solve that entire disciplines and scientific communities flourish solving subsets of these equations for particular applications. As complicated as this set of equations looks, it becomes even more complicated for high-temperature ionized flows and for multiphase flows. Several things make it difficult to solve the equations: lack of knowledge of the input parameters such as chemical reaction rates, physical diffusion coefficients, or boundary conditions; inadequate numerical methods to resolve the physical phenomena; and inadequate computer time and memory.

NUMERICAL METHODS

We have experimented with various different approaches for solving the coupled set of continuity equations representing fluid convection. These include both Eulerian and Lagrangian methods, implicit and explicit methods, with various types of adapting and moving computational grids. Here we describe our experience in terms of simulating flames.

For high-speed flows, that is, for Mach numbers greater than 0.5, we commonly use the latest versions of the Flux-Corrected Transport (FCT) algorithm (ref. 2,3). This is an explicit, nonlinear, monotone, Eulerian algorithm accurate to fourth-order in phase and second-order in time. FCT has been shown to provide highly accurate solutions for both subsonic and supersonic flows and effectively acts as a high-frequency filter for structures less than a few computational cells in size. It is a choice algorithm to use when sound waves must be resolved. There is a basic one-dimensional algorithm that can be extended by timestep-splitting and direction-splitting techniques to multidimensions, and there are also fully two-dimensional, three-dimensional, or finite-element versions (ref. 4,5). However, for very subsonic flames, we cannot afford either the computational expense of resolving sound waves or the potential loss of accuracy of an inordinately long calculation, and so an implicit method is needed. FCT, however, is essentially explicit and meanst to describe compressible flows.

Initially we thought that the fluid dynamics equations should be solved in a Lagrangian manner to be sure that the physical diffusion processes, which are crucial to a description of a flame, are well resolved and not washed out by even high-order residual numerical diffusion. It was this concern for accuracy and cost that led to the development of the implicit, Lagrangian algorithm, ADINC (ref. 6), and its application in a one-dimensional time-dependent flame model (ref. 7). At that time, we were also developing a new approach to multidimensional Lagrangian computations, SPLISH (ref. 8). This is a two-dimensional implicit Lagrangian algorithm that uses a mesh of dynamically restructuring triangles to avoid grid tangling and maintain high accuracy at interfaces. This algorithm was applied to a number of purely fluid-dynamic problems in wave propagation and droplet breakup (ref. 9), but due to its inherent complexity, has not yet been extended to flame computations. In particular, we found that there are inherently unstable properties associated with Lagrangian methods that make them less robust and therefore less generally useful than Eulerian methods.

The problem of what algorithm to use in multidimensions was solved with the conception and development of the Barely Implicit Correction to FCT, called BIC-FCT developed by Patnaik (ref. 11). BIC-FCT removes the timestep limit imposed by the sound speed by adding one implicit elliptic equation. The method is based on an analysis by Casulli and Greenspan that shows that it is not necessary to treat all terms in the fluid dynamic equations implicitly to use longer timesteps than allowed by explicit stability limits. Only the two terms which force the numerical stability limit need to be coupled and solved implicitly.

The BIC-FCT method solves the compressible, gas dynamic conservation equations for density ρ, momentum density ρv, and total energy density E, by a two-stage algorithm. The first stage is an explicit predictor method that determines the estimated new values $\tilde{\rho}$, $\tilde{v}$. The second step is an implicit correction step which produces δP, the additional pressure required to accelerate the fluid momentum from the explicit predictor

values, $\tilde{\rho}\tilde{\mathbf{v}}$, to the final implicitly corrected values, $\rho^n \mathbf{v}^n$. Because this correction deals with the sound waves (which were improperly computed by the explicit monotone predictor step in this algorithm) and not with the convection, there is no interference caused by the FCT algorithm. Only one elliptic equation must be solved to make the fluid equations implicit.

One particularly surprising aspect of this method is its relatively low cost: one implicit timestep using BIC-FCT takes about the same CPU time as one explicit FCT timestep, as measured on a CRAY-XMP. Normally we would have expected the implicit method to cost five to ten times more per timestep. This unexpected gains is partially primarily due to the fact that standard explicit implementation of FCT uses requires both a half-step prediction and a whole-step correction procedure each timestep. BIC-FCT does not split the timestep, but instead requires solving one finite-difference elliptic equation. The choice of a very fast multigrid method (ref. 12) to solve the elliptic equation is crucial to obtaining the computational speed. Tests of BIC-FCT in flame computations have shown that this algorithm is accurate enough to use in a flame model that also must resolve species' diffusion. Besides being a reasonable alternate to ADINC in one dimension, it generalizes in same straight-forward way FCT does to multidimensions and to any geometry used for the computational grid.

The specific algorithm we use to solve complex, stiff sets of ordering differential equations that represent the chemical reactions is CHEMEQ (ref. 13). CHEMEQ is a hybrid integrator that attempts to sort the stiff equations from the regular equations, and then apply a different solution method to each. For the stiff equations, an asymptotic method is used. For the regular equations, an explicit Euler method may be used. A great deal of effort has gone into optimizing this algorithm for vector and parallel computers has resulted in the VSAIM and TBA versions.

The solution of diffusion velocities for the individual species are obtained in several ways. Originally an arbitrarily accurate iterative algorithm was developed (ref. 14) and used. Recently a less expensive approach was taken that uses a Fickian term plus a correction (ref. 15). More details on the algorithms mentioned above and on algorithms for the solution of thermal conduction, thermal diffusion, and radiation terms can be found in refs. 1, 7, and 16.

Several generic approaches have evolved for solving sets of equations such as Eqs. (1) – (10) in which a number of different physical processes, represented by different types of mathematical terms, interact. The major methods are the global-implicit method, also called the block-implicit method and the fractional-step method, also called timestep splitting, and the various approaches are often combined into "hybrid" algorithms (ref. 1). Our method of choice has been timestep splitting because of its relatively straightforward applicability and its flexibility in incorporating the best available numerical algorithm for each particular physical process described in Table 1. In this approach, the individual processes are solved independently and the changes resulting from the separate partial calculations are coupled (added) together. The processes and the interactions among them may be treated by analytic, asymptotic, implicit, explicit, or other methods. Advantages of this approach are that it avoids many costly matrix operations and allows the best method to be used for each type of term.

Consider, for example, writing the coupled partial differential equations describing a flame as

$$\frac{d}{dt}\rho(\mathbf{x},t) \;=\; \mathrm{G}(\rho, \nabla\rho, \nabla\nabla\rho, \mathbf{x}, t) \tag{14}$$

where ρ is a vector, each component of which is a function of the time t and the vector position $\mathbf{x}$. Now rewrite this as

$$\frac{d}{dt}\rho(\mathbf{x},t) \;=\; \mathrm{G}_1 + \mathrm{G}_2 + \mathrm{G}_3 + \cdots + \mathrm{G}_M \;, \tag{15}$$

where G has been broken into its constituent processes. Each of the functions $\{\mathrm{G}_i\}$ contributes a part of the overall change in ρ during the numerical timestep. Thus

$$\left.\begin{aligned} \Delta\rho_1^{n-1} &= \Delta t\, \mathrm{G}_1^{n-1} \\ \Delta\rho_2^{n-1} &= \Delta t\, \mathrm{G}_2^{n-1} \\ \vdots \quad & \quad \vdots \\ \Delta\rho_M^{n-1} &= \Delta t\, \mathrm{G}_M^{n-1} \end{aligned}\right\} \tag{16}$$

For example, G_1^{n-1} might be the chemical kinetics terms, G_2^{n-1} the diffusion terms, G_3^{n-1} the thermal conduction terms, and so on. The solution for the new values ρ^n is found by summing all of the partial contributions,

$$\rho^n \;=\; \rho^{n-1} + \sum_{m=1}^{M} \Delta\rho_m^{n-1} \;. \tag{17}$$

If each of the processes is simulated individually, Eq. (17) gives a simple prescription for combining the results.

From our experiences developing and using computer programs for reactive flow problems, we have learned the type of coupling that must be used for problems in which the convective transport is implicit, such as

this case, or explicit, such as used for detonation problems, is somewhat different. This difference is based on different requirements of accuracy and stability. In computations with implicit convection, the changes in pressure (ref. 7) or internal energy (ref. 16) resulting from the individual processes are not incorporated into the solution as soon as they are computed, but instead are accumulated over the timestep. The entire change in internal energy is then added to the energy equation in the fluid convection step.

The algorithms used to solve the parts of the equations representing various physical processes in the computation each have their own timestep criterion for stability and accuracy. In flame calculations, the convection timestep as required by BIC-FCT is not the smallest. The actual overall timestep that is used is determined by the diffusive transport processes, which reduce the value of the timestep determined by the fluid velocity by at least a factor of five. To some extent, the effects of diffusive transport can be subcycled within the timestep, but if any variable changes more than about 15% during a timestep, the timestep must be reduced.

RESULTS OF FLAME SIMULATIONS

Importance of contributing processes

With so many processes contributing to the description of a flame, it is important to understand their relative importance under different circumstances. Here we summerize the work in ref. 18, which is a systematic study of the relative importance of various diffusive transport processes to the burning velocity in rich, lean, and stoichiometric hydrogen-air mixtures. These computations were performed with the one-dimensional flame model, FLAME1D (ref. 7), that uses the ADINC algorithm with a specially designed Lagrangian adaptive rezoning method, a detailed 25-step hydrogen-oxygen chemical reaction scheme, describing interactions of H_2, O_2, H_2O, H, O, OH, HO_2 and H_2O_2 (ref. 19) the full iterative solution of the species' diffusion equations, and algorithms for thermal conduction and thermal diffusion.

In the calculations described now, the model was configured with an open boundary at one end to simulate an unconfined system. All of the calclations were performed in a planar (Cartesian) geometry. The initial temperature and pressure of the mixture were 298 K and 1 atm, respectively. The flame was initiated by superimposing a Gaussian temperature profile with the central temperature and width chosen so that the added initial energy was above the minimum ignition energy for the flame to evolve into a steady profile.

For either thin or planar flames, the instantaneous normal burning velocity can be calculated from the flame velocity if we know the velocity of the unburned gases ahead of the flame. As shown in Fig. 1, for planar flames, the velocity of the unburned gases ahead of the flame is constant. Hence the burning velocity can be unambiguously determined as the difference between the flame velocity and the flow velocity ahead of the flame,

$$V_{\text{burn}} = V_{\text{flame}} - V_{\text{fluid}} \,. \tag{18}$$

The three diffusive transport processes considered were thermal conduction, molecular (ordinary) diffusion, and thermal diffusion. Calculations were performed with various combinations of these turned on or off for three mixtures of H_2, O_2, and N_2 which are fuel-lean 0.65:1:3.76, stoichiometric 2:1:3.76, and fuel-rich 15:1:3.76.

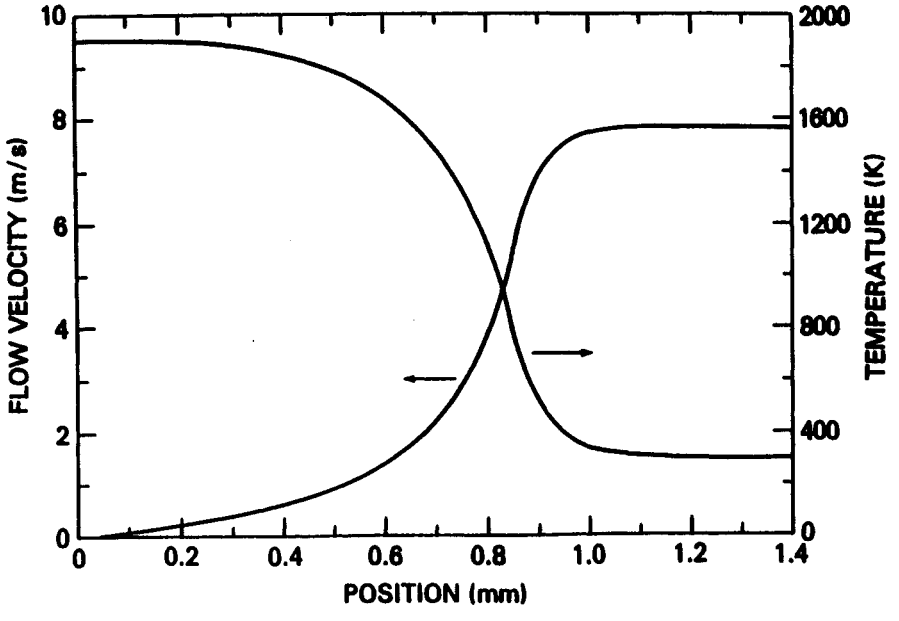

Figure 1. Velocity and temperature in a planar flame propagating in an H_2:O_2:N_2/2:1:4 mixture.

Table 2. Burning Velocities of H_2-Air Mixtures

Case	Processes On	Lean	Stoichiometric	Rich
(a)	All	36 cm/s	185 cm/s	44 cm/s
(b)	Thermal Conduction Ordinary Diffusion	40	195	48
(c)	Thermal Conduction	25	85	0
(d)	Ordinary Diffusion Thermal Diffusion	0	115	38

Table 2, which summarizes these results for four cases, shows that the relative importance of thermal diffusion does not change from lean to rich mixtures. Cases (a) and (b) shows that the effect of thermal diffusion is to lower burning velocities 6–11%. Hydrogen moves fast and its behavior dominates the diffusion properties of the system. It diffuses from the flame into the cold material by molecular diffusion. Thermal diffusion diffuses hydrogen from the lower-temperature region to the higher-temperature region. Thus, the two processes have an opposite effect. Thermal diffusion inhibits hydrogen movement into unreacted material and therefore when there is no thermal diffusion, the burning velocity increases. In stoichiometric mixtures, thermal conduction and molecular diffusion have about equal importance in determining the flame velocity. This is not true in lean or rich mixtures. In the lean mixture, thermal conduction is much more important, without it no steady burning velocity is reached. In the rich mixture, molecular diffusion is more important and without it, the flame does not propagate.

Evolution to cellular flame structure

Flames are subject to a number of different instabilities that originate in the competing effects of the controlling physical processes. Thermo-diffusive, Landau, and Rayleigh-Taylor instabilties lead, for example, to phenomena such as cellular structures at the flame front, differences in the shape and behavior of upward-propagating and downward-propagating flames, and the evolution of laminar to turbulent flames. These instabilities themselves are usually analyzed by a linear stability analysis of simplified sets of equations describing the balance between selected processes. However, the nonlinear effects are those which govern

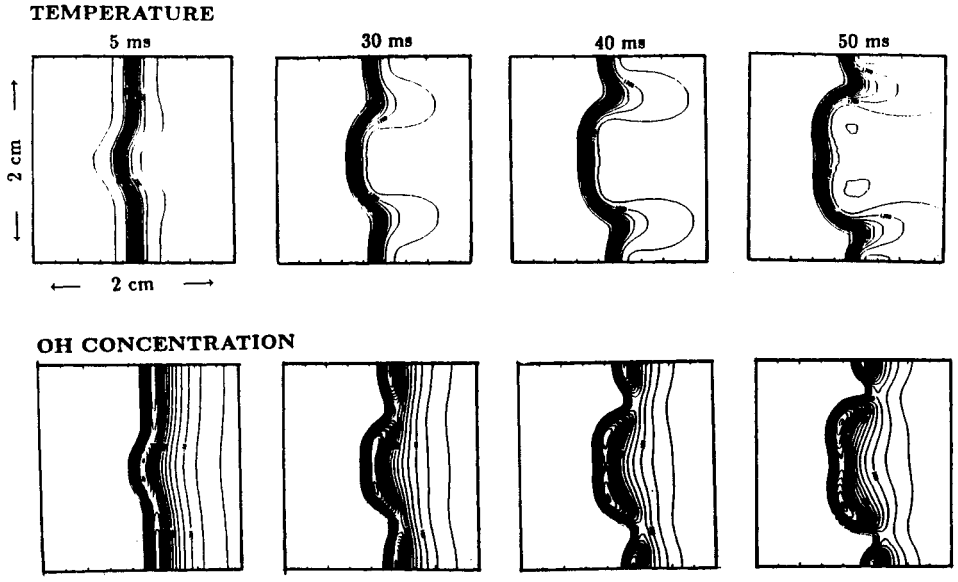

Figure 2. Temperature and OH number density contours for a flame propagating in a mixture of H_2:O_2:N_2 in the ratio 1.5:1:10, at the burning velocity of 12 cm/s, in the reference fram of the flame. The hot burned material (high temperature, high OH densities) are on the left, and the cold, unburned material (low temperature, low Oh density) are on the right. The initial perturbed flamefront develops progressively more structure.

the behavior after the initial onset of the instability, and sometimes the combined effects of a number of the controlling processes cannot be separated from each other in any simple way. In addition, sound waves in the system can act as both a means of propagating information and as a trigger of instabilities in the reacting flow.

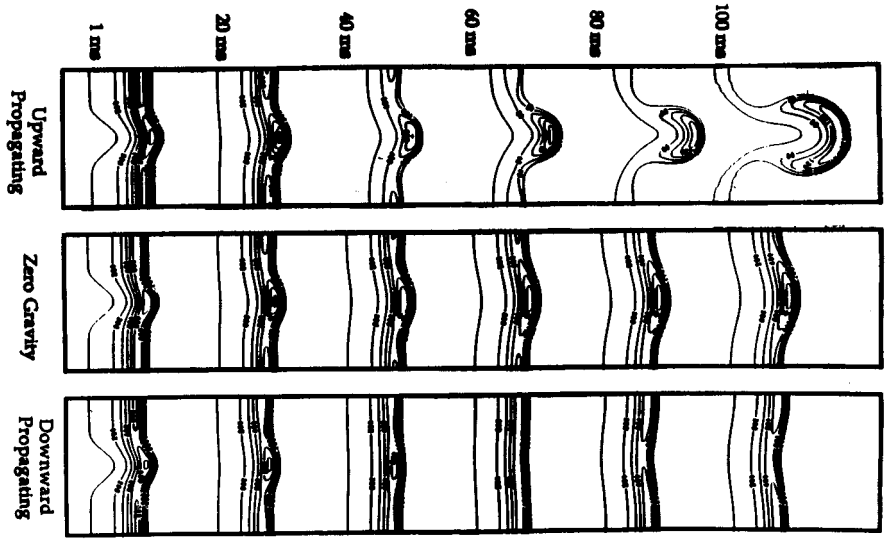

Figure 3. Comparison of OH number density contours in flames ain a hydrogen-oxygen-nitrogen mixture in the ratio 1:1:10.

Recent detailed two-dimensional time-dependent simulations of hydrogen-oxygen flames have started the process of isolating and studying the importance of various physical and chemical processes in determining the structure and stability of a multidimensional flame. These calculations use the FLIC2D model (ref. 16), which uses BIC-FCT, the full 25-step chemcial reaction mechanism, and includes molecular diffusion, thermal conduction, and gravity. The computations to date were performed in a reference frame moving at the one-dimensional laminar burning velocity. This burning velocity, and the initial unperturbed conditions of the flamefront, are determined from analogous one-dimensional calculations.

Figure 2, taken from the work by Patnaik et al. (ref. 20), shows the evolution of a lean zero-gravity hydrogen flame with the perturbation in the center, as shown in the first frame. In time, the structure at the front grows and forms into a cellular shape very similar to those seen experimentally. By the end of the computation, the cellular structure appears to be splitting again, but the computation had to be terminated because the flame was moving out of the finely gridded region and coming too close to the upper and lower walls. Simular computations in a rich hydrogen flame show that the instability is damped. Further simulations in the lean mixture with the hydrogen diffusion coefficient set equal to the oxygen diffusion coefficient show that the instability dies; but when the oxygen coefficient is set equal to the hydrogen coefficient, the instability persists. The results of the calculations support the idea that the diffusional-thermal instability is an important controlling mechamism in producing cellular structure in flames. This mechanism assumes that the process is controlled by the deficient component: for lean hydrogen mixtures, hydrogen is the limiting reactant and its mass diffusivity is greater than the thermal diffusivity of the mixture.

It is known from flammability studies that a flame propagating upward in a tube propagates in a wider range of mixture stoichiometries and dilutions than a flame propagating downward. This suggests a dependence on gravity that can be investigated with the detailed flame model described above. Figure 3 shows the evolution of a flame propagating upward, downward, and in zero gravity for the same lean mixture of hydrogen, oxygen, and nitrogen. The differences here are dramatic: the zero-gravity case shows a cellular structure forming; the upward-propagating flame becomes more and more curved until a buble is formed and seems to continue to grow; and the downward-propagating flame oscillates from concave to convex. These results have been explained based on combinations of the thermo-diffusive mechanism and a Rayleigh-Taylor instability (ref. 21).

An unstable, high-speed confined reacting flow

An extensive series of numerical simulations performed by Kailasanath (e.g., refs. 22 and 23) have shown that acoustic interactions in confined flows are crucial in determining the generation and merging of large-scale structures in the flow. These simulations use two-dimensional planar and axisymmetric versions of the explicit FCT algorithm. Selected calculations have been carried over hundreds of thousands of timesteps to obtain fluctuation spectra of selected variables. In a calculation over such a large physical domain with such a complex and changing fluid structure, it becomes prohibitive to resolve the structure of the flame. In this case, we have used a model of energy release based on the hydrogen-oxygen reaction mechanism to consider the effects of energy release on the flow.

Figure 4 shows a complicated axisymmetric flow in which a gas flows out of a long cylindrical inlet into a chamber of larger diameter. The exit condition from this larger chamber is choked flow so that the flow becomes sonic at the exit nozzle. The top portion of the figure shows a schematic of the chamber and the bottom portion shows a series of instantaneous streamlines of the flow in the cross-hatched region. Lines originating at the centers of vortices have been drawn between the streamlines to show the evolution of the vortex structures.

This calculations describes a subsonic high-speed slightly preheated mixture of hydrogen and air entering into a combustor. The mixture evolves into a quasi-periodic pattern as vortices were shed, merged, and exited through the nozzle. Temperature contours before ignition are essentially uniform, but showed the effects of compressibility. There is a strong coupling between the vortex structures formed in the shear layer and the acoustics in a ramjet combustion chamber. For example, the flowfield has an overall repetition cycle of 6000 steps, corresponding to a low-frequency mode of $\approx$ 150 Hz. In addition, the first vortex rollup appears with a frequency of $\approx$ 450 Hz. The low-frequency mode, corresponding to the quarter wave mode of the inlet, controls the overall merging pattern in the chamber. The higher frequency mode corresponds to the first longitudinal acoustic mode of the chamber.

Figure 5 is a continuation of a calculation similar to that in Figure 4, but after a time the mixture was "ignited" in a small region around the inlet (ref. 24). Chemical reactions and heat release are allowed to occur according to an induction parameter model. The instantaneous streamlines and temperature contours show the flame front moving down the chamber and a quasi-steady pattern is eventually set up. The flame front is located on the temperatue contours both by the the high temperatures and the dark lines caused by closely spaced contours. In time, the roll-up in the shear layer causes the reaction front to curve downward and engulf the cold mixture which subsequently burns. As the reaction moves downstream, a new vortex forms near the step between timesteps 175,000 and 180,000. This mixes the burned gases with the incoming mixture and acts as an ignition source. The flow field undergoes a cycle of roughly 25,000 timesteps, or 3.463 ms. The low-frequency mode persists in the reacting flow, but its amplitude is higher.

FUTURE DIRECTIONS

Two very different types of models have been described: the detailed models of the multispecies premixed gas-phase flames and the fluid model of a complex flow containing a flame. In the detailed model, a number of the contributing processes are modeled in as much detail as possible. In the fluid model, the processes not described by the fluid equations alone are approximated by a simple energy-release model. The differences in the levels of the models of the fluid dynamics, chemistry, and diffusive transport processes are necessary because of current and, no doubt, future limitations in the computer memory and speed available.

There are many ways to extend these calculations to describe, for example, more complex flows or to include more detailed or complex physical processes. For the purposes of this discussion, however, we consider only gas-phase problems that can be solved by adding more complex or additional physical processes or by using more efficient numerical software and hardware.

One major new direction this work can take is to simulate diffusion flames. As it is, the detailed model is ideally suited to simulate the time-dependent behavior of laminar diffusion flames. To date, Laskey (ref. 25) and Ellzey (ref. 26) have taken an intermediate approach: they have used the BIC-FCT algorithm as a basis for simulating axisymmetric diffusion flames with more complex fluid structures and approximate models of reactions and energy release. Time-dependent multidimensional detailed simulations, although now possible, have not yet been attempted. However, a very good set of steady-state computations have been done by Smooke (ref. 27) with detailed chemical kinetics.

There have also been a number of two-dimensonal and three-dimensional computations of transitional flows, that either have a very low Reynolds number or only attempt to resolve the large-scale structures in the flow. The purpose of these calculations is to determine the dynamics of the large structures and measure the mixing that occurs in the structures (e.g., refs. 28, 29). Some of these models have allowed energy to be released when a specified mixing level has been reached (e.g., refs. 29, 30).

Other extensions of these calculations are to more complex flows or more complex representation of the physical or chemical processes. This could apply to either premixed or diffusion flames. As the flow becomes more and more complex, the chemical reactions involve more species or more reaction pathways, or complex radiation or diffusive transport processes become important, the computations require more and more computer time and memory. At this stage, we need either more efficient algorithms to represent the processes or design faster or more clever computers. Dynamically adapting computational grids (e.g., refs. 5, 33) are one approach to reducing computer expense for the fluid portion of the calculation. More optimal timestep control on the integrators for stiff ordinary differential equations would reduce the time of chemical kinetics computations.

But a truly major breakthrough now will only come from use of new types of computers with radically new architectures. Consider, for example, the Connection Machine, a computer with thousands of interconnected processors connected in a hypercube configuration. With this computer, it is straightforward to have all of the processors working simultaneously, in parallel, on similar types of operations. Thus, for example, if each

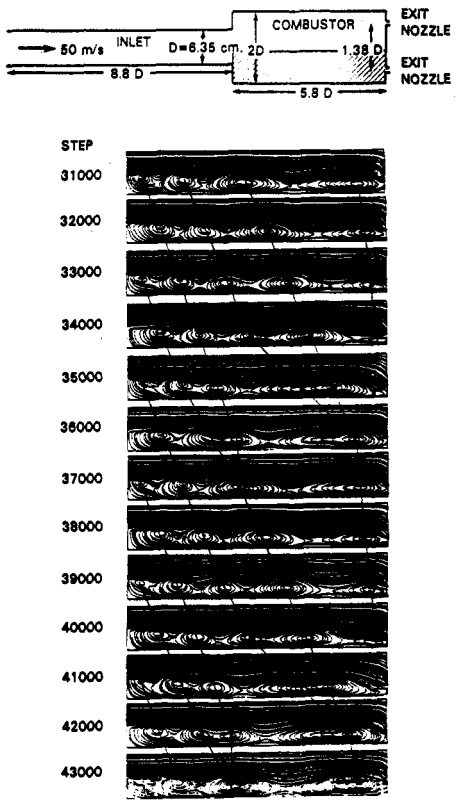

Figure 4. Top: Schematic of an axisymmetric flow with the line of symmetry through the center. Bottom: Calculated instantaneous velocity streamlines in the hatched region of the schematic. Lines through the streamlines connect the centers of vortex structures (refs. 22, 23)

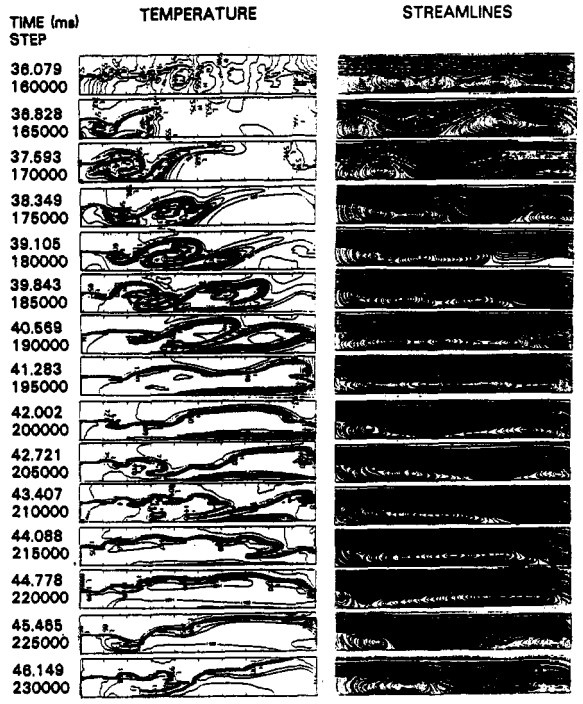

Figure 5. Instantaneous streamlines and temperature contours from a calculation of a reacting flow initiated in a cold flow similar to that shown in Fig. 4 (refs. 22, 23).

processor represents a fluid element, the flow at each element at the next timestep can be found at every fluid element at the same cost in computer time it would take to process the answer for one particular fluid element. Alternately, each processor could be integrating the chemical reaction equations in a given fluid element (ref. 33). Or another approach might be to use a heterogeneous computer system, which would use an entirely different computer, or a computer whose configuration can be altered, so that the best configuration of processors is used for the particular type of equation being solved. Adopting the simulations models to these architectures will make major breakthroughs in what we can calculate.

Acknowledgements

This paper reviews work done in collaboration with K. Kailasanath, Jay P. Boris, Theodore Young, and Gopal Patnaik. The author also wished to acknowledge collaborations with Janet Ellzey and Kenneth Laskey. The work has been funded by the Naval Research Laboratory through the Office of Naval Research and the National Aeronautic and Space Administration through the Microgravity Research Program.

REFERENCES

1. E.S. Oran and J.P. Boris, *Numerical Simulation of Reactive Flow*, Elsevier, New York, (1987).
2. J.P. Boris and D.L. Book, *Methods in Computational Physics*, 16, 85–129, Academic Press, New York (1976).
3. J.P. Boris, J.H. Gardner, E.S. Oran, S. Zalesak, J. Ellzey, G. Patnaik, D.L. Book, R.H. Guirguis, *LCPFCT – A Monotone Algorithm for Solving Continuity Equations*, to appear, Naval Research Laboratory Memorandum Report (1990).
4. S. Zalesak, *J. Comp. Phys.* 31: 335–362 (1979).
5. R. Löhner, K. Morgan, and O.C. Zienkiewicz, *Comput. Meth. Appl. Mech. Eng.* 51, 441–465 (1985); and R. Löhner, K. Morgan, M. Vahdati, J.P. Boris, and D.L. Book, submitted to *J. Comp. Phys.*.
6. J.P. Boris, *ADINC: An Implicit Lagrangian Hydrodynamics Code*, NRL Memorandum Report 4022, Naval Research laboratory, Washington, DC, 20375 (1979).
7. K. Kailasanath, E.S. Oran, and J.P. Boris, *A One-Dimensional Time-Dependent Model for Flame Initiation, Propagation, and Quenching*, NRL Memorandum Report 4910, Naval Research laboratory, Washington, DC, 20375 (1982).
8. M.J. Fritts and J.P. Boris, *J. Comput. Phys.* 31, 173–215 (1979).
9. D.E. Fyfe, E.S. Oran, and M.J. Fritts, *J. Comput. Phys.* 76, 349–384 (1988).
10. G. Patnaik, R.H. Guirguis, J.P. Boris, and E.S. Oran, *J. Comp. Phys.*, 71, 1–20, (1987).
11. V. Casulli and D. Greenspan, *Int. J. Num. Meth. Fluids* 4, 1001–1012 (1984).
12. C.R. DeVore, *Vectorization and Implementation of an Efficient Multigrid Algorithm for the Solution of Elliptic Partial Differential Equations*, NRL Memorandum Report 5504, Naval Research Laboratory, Wash., D.C., 20375 (1984).
13. T.R. Young, and J.P. Boris, *J. Phys. Chem.* 81, 2424–2427 (1977); also T.R. Young, *CHEMEQ: Subroutine for Solving Stiff Ordinary Differential Equations*, Naval Research Laboratory Memorandum Report 4091, Naval Research Laboratory, Wash., D.C., 20375 (1979).
14. W.W. Jones and J.P. Boris, *Comput. Chem.*, 5, 139–146 (1981).
15. R.J. Kee, G. Dixon-Lewis, J. Warnatz, M.E. Coltrin, and J.A. Miller, *A Fortran Computer Code Package for the Evaluation of Gas-Phase Multi-Component Transport Properties*, Report SAND86-8243, Sandia National Laboratories, Livermore, CA (1986).
16. G. Patnaik, K.J. Laskey, K. Kailasanath, E.S. Oran, and T.A. Brun, *FLIC – A Detailed, Two-Dimensional Flame Model*, to appear as NRL Memorandum Report, Naval Research Laboratory, Wash., D.C., 20375
17. N.N. Yanenko, *The Method of Fractional Steps*, Springer-Verlag, New York (1971).
18. K. Kailasanath and E.S. Oran, in *Complex Chemical Reaction Systems*, eds. J. Warnatz and W. Jager, 243–252, Springer-Verlag, New York (1987).
19. T.L. Burks and E.S. Oran, *A Computational Study of the Chemical Kinetics of Hydrogen Combustion*, Naval Research Laboratory Memorandum Report 4446, Naval Research Laboratory, Wash., D.C., 20375 (1981).
20. G. Patnaik, K. Kailasanath, E.S. Oran, and K.J. Laskey, *Twenty-Second Symposium (International) on Combustion*, 1517–1526, The Combustion Institute, Pittsburgh (1988).
21. K. Kailasanath, G. Patnaik, and E.S. Oran, *Effect of Gravity on Muldidimensional Laminar Premixed Flame Structure*, IAF-88-354, International Astronautical Federation, Paris (1988).
22. K. Kailasanath, J.H. Gardner, J.P. Boris, and E.S. Oran, *J. Prop. Power*, 3, 525–533 (1987).
23. K. Kailasanath, J.H. Gardner, J.P. Boris, and E.S. Oran, 5, 165–171 (1989).
24. K. Kailasanath, J.H. Gardner, E.S. Oran, and J.P. Boris, submitted to *Combus. Flame* (1989).
25. K.J. Laskey, J.L. Ellzey, G. Patnaik, and E.S. Oran, *A Numerical Study of a Turbulent Diffusion Flame*, AIAA Paper No. 89-0572, American Institute of Aeronautics and Astronautics, Washington, DC, 1989.
26. J.L. Ellzey, K.J. Laskey, and E.S. Oran, submitted to the *Proceedings of the 12th International Colloquium on the Dynamics of Explosions and Reactive Systems*, to appear in *Progress in Aeronautics and Astronautics*, AIAA, Washington, 1989.
27. M.D. Smooke, in *Numerical Approaches to Combustion Modeling*, eds. E.S. Oran and J.P. boris, AIAA, Washington, DC, to appear (1990).

28. F.F. Grinstein, E.S. Oran, and J.P. Boris, *J. Fluid Mech.* 165, 201–220 (1986).
29. F.F. Grinstein, R.H. Guirguis, E.S. Oran, and A.K.M.F. Hussain, *Three-Dimensional Numerical Simulation of a Compressible, Spatially Evolving Mixing Layer*, AIAA Paper Number AIAA-88-0042, AIAA (1988).
30. G. Heidarinejad and A.F. Ghoniem, AIAA Paper 89-0573, American Institute of Aeronautics and Astronautics, Washington, DC (1989). AIAA Paper 89-0573 (1989); also A.F. Ghoniem and P. Givi, *AIAA J.*, 26, 690-697 (1988).
31. P.A. McMurtry, J.J. Riley, and R.W. Metcalfe, *J. Fluid Mech.* 199, 297-332 (1989).
32. M.J. Berger and A. Jameson, in *9th Int. Conf. Num. Metho. Fluid Dyn.* Springer, New York (1985).
33. E.S. Oran, J.P. Boris, and E. Brown, *Fluid Dynamics on a Connection Machine – Preliminary Timings and Complex Boundary Conditions*, to appear as AIAA Paper (1990).